STRUCTURAL CHEMISTRY

ISSN 2053-2296

Synthesis, crystal structure and solution behaviour of a tetranuclear cyclometalated nickel(II) thiolate complex with a puckered Ni_4S_4 ring

Masakazu Hirotsu,* Ryota Futaki and Momoka Yasuda

Department of Chemistry, Faculty of Science, Kanagawa University, Kanagawa-ku, Yokohama 221-8686, Japan. *Correspondence e-mail: mhiro@kanagawa-u.ac.jp

Received 26 October 2026
Accepted 16 November 2026

Edited by I. D. Williams, Hong Kong University of Science and Technology, Hong Kong

Keywords: crystal structure; nickel(II) complex; thiolate; cyclometalation; N,C,S-tridentate ligand; cyclic voltammetry.

CCDC reference: 2603547

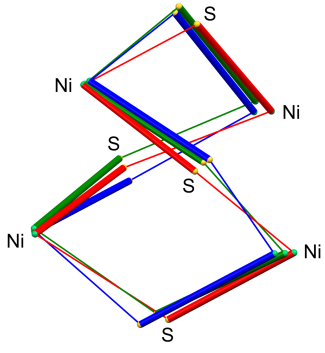
Supporting information: this article has supporting information at journals.iucr.org/c

The tetranuclear cyclometalated nickel(II) thiolate complex tetrakis(μ_2-{(*Z*)-2-[2-(quinolin-8-yl)eth-1-en-2-id-1-yl]benzenethiolato(2−)-$\kappa^4N,C^1,S:S$}tetranickel(II) dichloromethane disolvate, $[Ni_4(C_{17}H_{11}NS)_4]\cdot 2CH_2Cl_2$ (**1**·$2CH_2Cl_2$), was synthesized by the reaction of 8-(benzo[*b*]thiophen-2-yl)quinoline (**2**) with $[Ni(cod)_2]$ (cod = 1,5-cyclooctadiene) *via* C—S bond cleavage. The $Ni(C_{17}H_{11}NS)$ unit in **1** consists of a nickel(II) ion and a dianionic N,C,S-tridentate ligand. The thiolate S atom bridges two Ni centres to furnish a puckered Ni_4S_4 ring with elongated Ni—S bonds between the units, due to the *trans* influence of the C-donor atom. The electrochemical and spectroscopic properties of **1** suggest that the tetranuclear structure is preserved in non-coordinating solvents under inert atmospheric conditions.

1. Introduction

Cyclometalation *via* chelation-assisted bond activation provides organometallic compounds with a strong metal–carbon bond. Group 10 pincer complexes with cyclometalated tridentate ligands have been extensively studied as catalysts, photosensitizers, light-emitting materials and drugs (Albrecht & van Koten, 2001; Niu *et al.*, 2011; Chakraborty *et al.*, 2015; Moreth *et al.*, 2025; Wu *et al.*, 2021). Furthermore, there is an increasing demand for the use of earth-abundant and inexpensive nickel complexes (Arora *et al.*, 2021; Gafurov *et al.*, 2021; John *et al.*, 2026). The pincer platform is particularly useful for the development of nickel complexes because the meridional coordination mode enhances the stability of otherwise labile nickel species (Grove *et al.*, 1983).

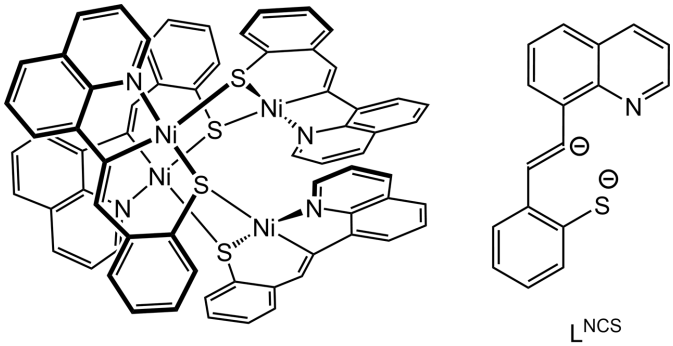
The first reported ligands with a pincer architecture were symmetrical with P,C,P- or N,C,N-donor atoms (Moulton *et al.*, 1976; van Koten *et al.*, 1978; Grove *et al.*, 1983). Because the electronic effects of the pincer ligands are largely attributed to the type of heterodonor atoms, such as N, P and S, unsymmetrical pincer complexes have also been investigated to unveil unique properties (Gafurov *et al.*, 2021). We have prepared N,C,S-pincer complexes of iron, ruthenium and rhodium using dibenzothiophene, benzothiophene and thiophene derivatives bearing N-heterocycles (Shibue *et al.*, 2008; Hirotsu *et al.*, 2011; Hirotsu *et al.*, 2012; Matsunaga *et al.*, 2017; Masuda *et al.*, 2020). The C—S bond of the thiophene ring undergoes oxidative addition reactions with low-valent metal complexes, such as metal carbonyls, to form two cyclometalated rings: an S-containing six-membered ring and an N-containing five-membered ring. On the other hand, P,C,S-pincer iron complexes derived from diphenylphosphine-substituted benzothiophene have also been reported (Hooper



OPEN ACCESS
Published under a CC BY 4.0 licence

et al., 2023). The π-acceptor properties of the phosphane P atom in the P,C,S-pincer system contrast with those of the less π-accepting sp^2 N-donor sites in our studies; to address this issue, the N-donor moiety can be modified by the introduction of a diazine ring (Futaki *et al.*, 2025). To further elucidate the N,C,S-pincer system, the characteristics of Group 10 metal complexes are of particular interest because of their reactivity.

In this article, we report a tetrameric N,C,S-pincer nickel(II) complex, [{Ni(L^{NCS})}$_4$] (**1**), where L^{NCS} is a doubly deprotonated form of 2-[2-(quinolin-8-yl)ethenyl]benzenethiol (Scheme 1). The crystal structure of **1** features a thiolate-bridged Ni_4S_4 ring structure. The solution behaviour of this complex was investigated by NMR spectroscopy, electronic absorption spectroscopy and cyclic voltammetry.



1

Scheme 1

Table 1
Experimental details.

Crystal data	
Chemical formula	$[Ni_4(C_{17}H_{12}NS)_4]\cdot 2CH_2Cl_2$
M_r	1450.00
Crystal system, space group	Tetragonal, $I4_1/a$
Temperature (K)	120
a, c (Å)	16.649 (3), 41.225 (7)
V (Å^3)	11427 (5)
Z	8
Radiation type	Mo $K\alpha$
μ (mm^{-1})	1.68
Crystal size (mm)	0.07 × 0.06 × 0.04
Data collection	
Diffractometer	Rigaku AFC11 with Saturn 724+ CCD
Absorption correction	Multi-scan (*REQAB*; Rigaku, 1998)
T_{min}, T_{max}	0.902, 1.000
No. of measured, independent and observed [$I > 2\sigma(I)$] reflections	93479, 6553, 5818
R_{int}	0.054
(sin $\theta/\lambda)_{max}$ (Å^{-1})	0.649
Refinement	
$R[F^2 > 2\sigma(F^2)]$, $wR(F^2)$, S	0.057, 0.151, 1.14
No. of reflections	6553
No. of parameters	408
No. of restraints	2
H-atom treatment	H atoms treated by a mixture of independent and constrained refinement
$\Delta\rho_{max}$, $\Delta\rho_{min}$ (e Å^{-3})	1.63, −0.70

Computer programs: *CrystalClear* (Rigaku, 2008), *SIR97* (Altomare *et al.*, 1999), *SHELXL2019* (Sheldrick, 2015), *ORTEP-3 for Windows* (Farrugia, 2012) and *Mercury* (Macrae *et al.*, 2020) and *WinGX* (Farrugia, 2012).

2. Experimental

2.1. General procedures

NMR spectra were recorded on a JEOL ECA-400 or a JEOL ECZ-600 spectrometer at room temperature. Elemental analysis was performed by A Rabbit Science Co. Ltd. UV–Vis spectra were measured on a JASCO V-770 spectrometer. Cyclic voltammetry measurements were performed at room temperature using an ECstat-302 potentio/galvanostat analyzer (EC Frontier Co. Ltd) under a nitrogen atmosphere.

2.2. Synthesis and crystallization

2.2.1. Preparation of 8-(benzo[*b*]thiophen-2-yl)quinoline (2)

8-(Benzo[*b*]thiophen-2-yl)quinoline (**2**) was prepared according to literature procedures and the ^{1}H NMR spectrum ($CDCl_3$) was consistent with the reported data (Masuda *et al.*, 2020; Brodnik *et al.*, 2016). ^{1}H NMR (400 MHz, C_6D_6): δ 6.75 (*dd*, J = 8.3, 4.1 Hz, 1H), 7.12 (*ddd*, J = 8.2, 7.2, 1.1 Hz, 1H), 7.15 (*m*, 1H), 7.21 (*ddd*, J = 8.2, 7.2, 1.0 Hz, 1H), 7.28 (*dd*, J = 8.1, 1.3 Hz, 1H), 7.49 (*dd*, J = 8.3, 1.8 Hz, 1H), 7.70–7.75 (*m*, 2H), 7.97 (*dd*, J = 7.3, 1.4 Hz, 1H), 8.20 (*d*, J = 0.4 Hz, 1H), 8.80 (*dd*, J = 4.1, 1.8 Hz, 1H). ^{1}H NMR (400 MHz, pyridine-d_5): δ 7.36–7.45 (*m*, 3H), 7.59 (*t*, J = 7.8 Hz, 1H), 7.82 (*dd*, J = 7.4, 1.4 Hz, 1H), 7.97 (*m*, 1H), 8.05 (*m*, 1H), 8.19 (*dd*, J = 8.3, 1.8 Hz, 1H), 8.35 (*dd*, J = 7.4, 1.4 Hz, 1H), 8.44 (*s*, 1H), 9.14 (*dd*, J = 4.1, 1.8 Hz, 1H). ^{1}H NMR [400 MHz, dimethyl sulfoxide-d_6 (DMSO-d_6)]: δ 7.34–7.42 (*m*, 2H), 7.66 (*dd*, J = 8.3, 4.1 Hz, 1H), 7.73 (*t*, J = 7.8 Hz, 1H), 7.92 (*m*, 1H), 7.99–8.05 (*m*, 2H), 8.31 (*s*, 1H), 8.40 (*dd*, J = 7.4, 1.3 Hz, 1H), 8.48 (*dd*, J = 8.3, 1.8 Hz, 1H), 9.07 (*dd*, J = 4.1, 1.8 Hz, 1H).

2.2.2. Preparation of [{Ni(L^{NCS})}$_4$] (1)

This complex was prepared in a nitrogen-filled glovebox. Compound **2** (52 mg, 0.2 mmol) and [Ni(cod)$_2$] (cod = 1,5-cyclooctadiene) (55 mg, 0.2 mmol) were dissolved in tetrahydrofuran (THF; 6 ml) below 10 °C and stirred for 30 min. The resulting red–brown suspension was stirred at 25 °C for 12 h. After addition of diethyl ether (40 ml), the dark-brown precipitate of **1** was collected by filtration, washed with diethyl ether (10 ml) and then dried under reduced pressure (yield: 57 mg, 89%).

^{1}H NMR (400 MHz, $CDCl_3$): δ 5.97 (*s*, 1H, Fe—C═CH), 6.61 [*dd*, J = 5.3, 7.9 Hz, 1H, C(quinolinyl, 3)—H], 6.65 [*m*, 1H, C(quinolinyl, 5)—H], 6.90–6.95 [*m*, 3H, C(quinolinyl, 6)—H, C(benzenethiolate)—H], 7.07 [*t*, J = 7.6 Hz, 1H, C(benzenethiolate)—H], 7.52 [*d*, J = 7.8 Hz, 1H, C(benzenethiolate)—H], 8.02 [*d*, J = 7.9 Hz, 1H, C(quinolinyl, 4)—H], 8.60 [*d*, J = 4.8 Hz, 1H, C(quinolinyl, 2)—H], 8.97 [*m*, 1H, C(quinolinyl, 7)—H]. ^{1}H NMR (600 MHz, C_6D_6): δ 6.17 (*s*, 1H), 6.21 (*dd*, J = 7.9, 5.2 Hz, 1H), 6.76 (*dd*, J = 7.7, 1.2 Hz, 1H), 6.77–6.83 (*m*, 2H), 6.88 (*ddd*, J = 8.0, 6.9, 1.4 Hz, 1H), 6.94 (*m*, 1H), 7.08 (*dd*, J = 7.5, 1.4 Hz, 1H), 7.38 (*dd*, J = 8.0, 1.1 Hz, 1H), 8.83 (*dd*, J = 5.2, 1.2 Hz, 1H), 9.42 (*d*, J = 7.8 Hz, 1H). ^{1}H NMR

Table 2
Selected geometric parameters (Å, °).

Ni1—C8	1.906 (3)	Ni2—C25	1.908 (3)
Ni1—N1	1.935 (3)	Ni2—N2	1.936 (3)
Ni1—S1	2.1320 (9)	Ni2—S2	2.1308 (8)
Ni1—S2^{i}	2.3241 (9)	Ni2—S1	2.3217 (9)
C8—Ni1—N1	86.20 (12)	C25—Ni2—S2	94.62 (10)
C8—Ni1—S1	94.33 (10)	N2—Ni2—S2	173.32 (8)
N1—Ni1—S1	175.18 (8)	C25—Ni2—S1	171.13 (9)
C8—Ni1—S2^{i}	171.21 (9)	N2—Ni2—S1	93.31 (8)
N1—Ni1—S2^{i}	93.42 (8)	S2—Ni2—S1	85.15 (3)
S1—Ni1—S2^{i}	85.33 (3)	Ni1—S1—Ni2	121.13 (4)
C25—Ni2—N2	85.90 (12)	Ni2—S2—Ni1^{i}	121.96 (4)

Symmetry code: (i) $-x+1, -y+\frac{1}{2}, z$.

(400 MHz, pyridine-d_5): δ 7.10 (*dd*, *J* = 5.1, 8.1 Hz, 1H), 7.16 (*m*, 2H), 7.34 (*d*, *J* = 4.7 Hz, 1H), 7.54–7.63 (*m*, 2H), 7.76 (*m*, 1H), 7.93 (*s*, 1H), 8.15 (*m*, 1H), 8.19 (*d*, *J* = 8.1 Hz, 1H), 8.38 (*d*, *J* = 7.0 Hz, 1H). ^{1}H NMR (400 MHz, DMSO-d_6): δ 6.87 (*m*, 2H), 7.07 (*s*, 1H), 7.29 (*d*, *J* = 6.8 Hz, 1H), 7.51 (*d*, *J* = 7.2 Hz, 1H), 7.55–7.63 (*m*, 2H), 7.78 (*d*, *J* = 7.8 Hz, 1H), 8.18 (*d*, *J* = 7.2 Hz, 1H), 8.54 (*d*, *J* = 8.2 Hz, 1H), 8.67 (*d*, *J* = 4.6 Hz, 1H). ^{13}C{^{1}H} NMR (100 MHz, $CDCl_3$): δ 118.9, 122.0, 122.5, 123.5, 125.5, 126.7, 127.2, 128.4, 131.4, 131.9, 132.7, 134.9, 137.4, 142.4, 148.3, 149.8, 150.8. UV–Vis (CH_2Cl_2): λ_{max}/nm (ε/dm^3 mol^{-1} cm^{-1}) 246 (135000), 282 (77000, shoulder), 365 (42500), 430 (23000, shoulder). Analysis calculated (%) for $C_{68}H_{44}N_4Ni_4S_4$: C 63.80, H 3.46, N 4.38; found: C 63.63, H 3.45, N 3.99.

The product can be recrystallized from dichloromethane–diethyl ether or *o*-dichlorobenzene–diethyl ether. Crystals of **1** suitable for X-ray diffraction analysis were grown from a dichloromethane solution.

2.3. Refinement

Details of the crystal data, data collection and structure refinement are summarized in Table 1. A dichloromethane molecule was modelled to be disordered over two positions, with occupancy factors of 0.85 and 0.15. H atoms were placed at calculated positions, with aromatic C—H = 0.95 Å and methylene C—H = 0.99 Å, and refined using a riding model with U_{iso}(H) = 1.2U_{eq}(C), except for the 2-positioned H atoms on the quinoline rings, which are involved in short contacts potentially associated with hydrogen bonding. These H atoms were found in the difference Fourier map and refined isotropically.

3. Results and discussion

3.1. Synthesis of complex 1

Treatment of 8-(benzo[*b*]thiophen-2-yl)quinoline (**2**) with [Ni(cod)$_2$] (cod = 1,5-cyclooctadiene) in THF at room temperature produced the tetranuclear nickel(II) complex [{Ni(L^{NCS})}$_4$] (**1**) in good yield, in which L^{NCS} is an N,C,S-tridentate ligand derived from **2** *via* C—S bond cleavage. Although complex **1** can be handled in air in the solid state, it rapidly decomposes in solution under aerobic conditions to regenerate **2** (Fig. 1). In contrast, the corresponding reaction of 2-(dibenzo[*b*,*d*]thiophen-4-yl)pyridine (**3**; Fig. 1) with [Ni(cod)$_2$] left most of **3** unreacted under the same conditions, suggesting that **3** is more resistant to cyclometalation *via* C—S bond cleavage than is **2**.

3.2. Structure of complex 1

Complex **1** crystallizes as a CH_2Cl_2 solvate in the tetragonal space group $I4_1/a$ (No. 88) with a half molecule of **1** and a CH_2Cl_2 molecule in the asymmetric unit (Figs. 2 and 3). The complete molecule of **1**, which is generated by the symmetry operation $(-x+1, -y+\frac{1}{2}, z)$, has a tetrameric structure consisting of four Ni(L^{NCS}) units. The L^{NCS} ligand acts as a tridentate ligand, ligated through its N, C and S atoms. The fourth coordination site at Ni is occupied by the thiolate S

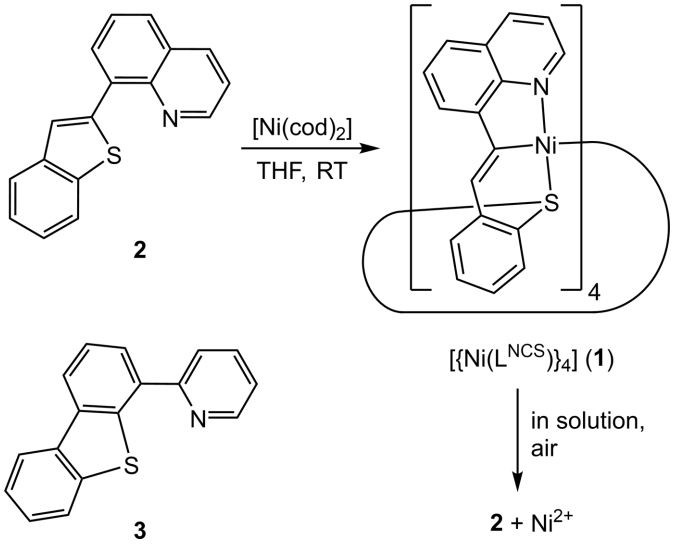


Figure 1
The structures of ligand precursors **2** and **3**, and the reaction of **2**.

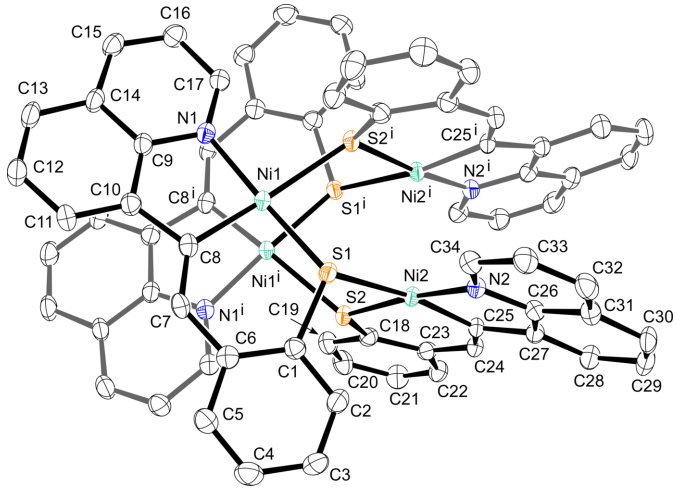


Figure 2
Perspective view of **1**, with displacement ellipsoids drawn at the 50% probability level. H atoms have been omitted for clarity. [Symmetry code: (i) $-x+1, -y+\frac{1}{2}, z$.]

Table 3
Hydrogen-bond geometry (Å, °).

D—H···A	D—H	H···A	D···A	D—H···A
C17—H17···S2^{i}	0.98 (3)	2.50 (3)	3.182 (3)	126 (2)
C34—H34···S1	0.99 (4)	2.52 (4)	3.174 (3)	124 (3)

Symmetry code: (i) $-x+1, -y+\frac{1}{2}, z$.

atom of another Ni(L^{NCS}) unit to form an Ni—S bond and thus complete a square-planar coordination geometry. The geometric parameters around Ni1 and Ni2 are comparable to each other (Table 2). Two sets of the face-to-face dimer of Ni(L^{NCS}) (Ni1/Ni1^{i} and Ni2/Ni2^{i}) are linked to each other through Ni—S bonds, giving the tetrameric molecule [{Ni(L^{NCS})}$_4$]. Thiolate-bridged tetrameric structures similar to **1** have been reported for [{Ni(L^{CNS})}$_4$] with C,N,S-tridentate ligands (Kawamoto & Kushi, 2004) and [{Ni(L^{ONS})}$_4$] with O,N,S-tridentate ligands (Bag & Pal, 2022), where L^{CNS} is 2-[(2,4-dichlorobenzylidene)amino]benzenethiolate(2−) and L^{ONS} is 2-{[(2-mercaptophenyl)imino]methyl}-6-methoxyphenolate(2−). The Ni(L^{NCS}) unit in **1** adopts an almost planar geometry; the r.m.s. deviation of the fitted atoms from the mean plane including the two chelate rings (Ni1/S1/N1/C1/C6–C10 and Ni2/S2/N2/C18/C23–C27) is 0.067 Å. The interplanar angles for the cofacial pairs of the Ni(L^{NCS}) units are 16.02 (4) and 16.08 (4)°, which are larger, respectively, than those of [{Ni(L^{CNS})}$_4$] and [{Ni(L^{ONS})}$_4$] (0.1–6.0°) (Kawamoto & Kushi, 2004; Bag & Pal, 2022). Relatively short (quinoline) C—H···S contacts are found between the Ni(L^{NCS}) units in a molecule, with H···S distances of 2.52 (4) and 2.50 (3) Å (Fig. 3 and Table 3).

The four Ni—S—Ni bridging structures in **1** construct a puckered Ni$_4$S$_4$ ring (Figs. 2 and 3). Similar thiolate-bridged cyclic structures, M_4S_4 (M is a transition metal), have been reported for Group 10 metal complexes. The palladium(II) complexes (Pd$_4$S$_4$) contain C,N,S-tridentate ligands (Kawamoto *et al.*, 1996; Kawamoto *et al.*, 2003), O,N,S-tridentate ligands (Roy *et al.*, 2009; Moosun *et al.*, 2016), or an S,N,S-tridentate ligand (Ataie *et al.*, 2025). The platinum(II) complexes (Pt$_4$S$_4$) contain C,N,S-tridentate ligands (Kawamoto *et al.*, 1996; Kawamoto *et al.*, 1997). However, a pincer unit containing a central C-donor atom has been applied to the M_4S_4 cyclic structures for the first time in this study. Therefore, the geometrical parameters of the Ni$_4$S$_4$ ring for **1** were compared with those of [{Ni(L^{CNS})}$_4$] and [{Ni(L^{ONS})}$_4$], and the results are summarized in Table 4. To visualize the differences, the Ni$_4$S$_4$ rings of these complexes are overlaid in Fig. 4. The differences between the intra-unit and inter-unit Ni—S bond lengths in **1** (0.19 Å) are larger than those in [{Ni(L^{CNS})}$_4$] and [{Ni(L^{ONS})}$_4$], which can be attributed to the *trans* influence of the C-donor atom in the L^{NCS} ligand. The S—Ni—S and Ni—S—Ni angles in **1** are smaller and larger than those in the analogous Ni$_4$S$_4$ rings. The Ni···Ni distances in **1** [2.9639 (9) and 2.9486 (9) Å] are shorter than those of [{Ni(L^{CNS})}$_4$] and [{Ni(L^{ONS})}$_4$], although no bonding interactions are suggested (Kawamoto & Kushi, 2004; Bag & Pal, 2022).

Table 4
Geometric parameters (Å, °) for Ni$_4$S$_4$ rings.

	[{Ni(L^{NCS})}$_4$] (**1**)	[{Ni(L^{CNS})}$_4$]^{a}	[{Ni(L^{ONS})}$_4$]^{b}
Ni—S^{c}	2.1320 (9), 2.1308 (8)	2.213 (18), 2.233 (19)	2.1446 (9)–2.1535 (9)
Ni—S^{d}	2.3241 (8), 2.3217 (9)	2.209 (18), 2.184 (18)	2.2211 (9)–2.2448 (9)
S—Ni—S	85.33 (3), 85.15 (3)	95.0 (7), 95.6 (7)	90.36 (3)–90.95 (3)
Ni—S—Ni	121.13 (4), 121.96 (4)	111.4 (8), 115.0 (8)	112.02 (4)–123.32 (4)
Ni···Ni	2.9639 (9), 2.9486 (9)	3.10 (1), 3.09 (1)	2.9807 (8), 3.0327 (7)

Notes and references: (*a*) Kawamoto & Kushi (2004); (*b*) Bag & Pal (2022); (*c*) intra-unit bond lengths; (*d*) inter-unit bond lengths.

In the crystal structure of **1**, intermolecular π–π stacking interactions exist between the quinoline rings of neighbouring molecules (Figs. 3 and 5). The distance between the two centroids of the C9–C14 (at x, y, z) and C26–C31 (at $y+\frac{1}{4}$, $-x+\frac{5}{4}$, $z+\frac{1}{4}$) rings is 3.748 Å. The interplanar separation is 3.58 Å and the angle between the planes is 3.66°. The benzenethiolate moieties do not contribute to the stacking interactions, and the void space between these moieties is occupied by a CH_2Cl_2 molecule.

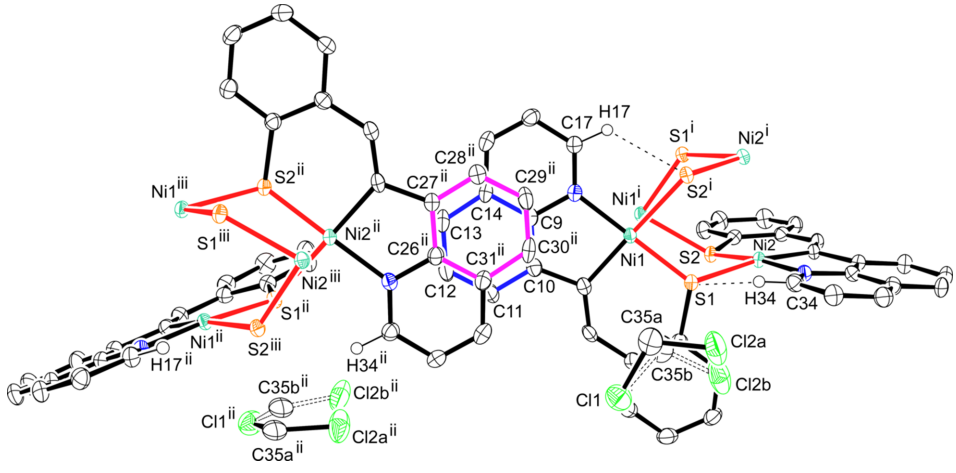


Figure 3
View of the Ni$_4$S$_4$ ring (red) in the CH_2Cl_2 solvate of **1** and the π–π stacking interaction between the C9–C14 (blue) and C26^{ii}–C31^{ii} (magenta) rings. The half molecule of **1**, excluding the Ni and S atoms, and H atoms have been omitted for clarity, except for the 2-positioned H atoms on the quinoline rings. [Symmetry codes: (i) $-x+1, -y+\frac{1}{2}, z$; (ii) $y+\frac{1}{4}, -x+\frac{5}{4}, z+\frac{1}{4}$; (iii) $-y+\frac{3}{4}, x+\frac{1}{4}, z+\frac{1}{4}$.]

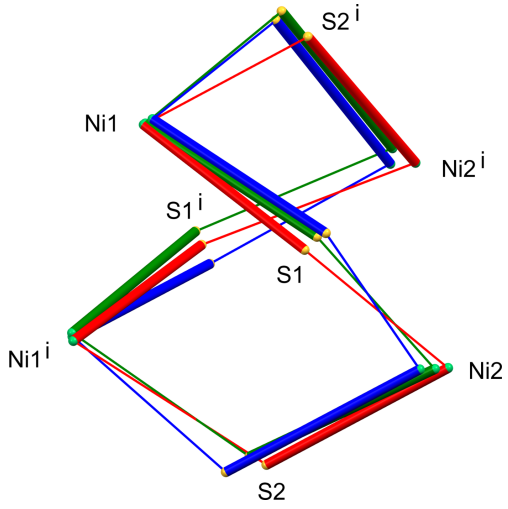


Figure 4
Overlays of the Ni_4S_4 ring structures of **1** (red), [{Ni(L^{CNS})}$_4$] (blue) (Kawamoto & Kushi, 2004) and [{Ni(L^{ONS})}$_4$] (green) (Bag & Pal, 2022). The atom labels are given for **1**. Intra-unit and inter-unit Ni—S bonds are drawn as thick and thin lines, respectively. [Symmetry code: (i) $-x+1$, $-y+\frac{1}{2}$, z.]

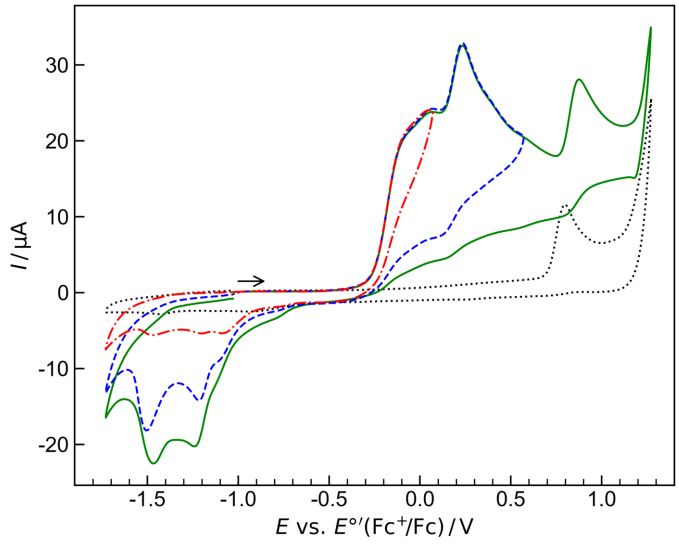


Figure 6
Cyclic voltammograms of **1** (5.0×10^{-4} *M*) with different switching potentials (0.07 V, red dashed–dotted line; 0.57 V, blue dashed line; 1.27 V, green line) and **2** (5.0×10^{-4} *M*, black dotted line) in CH_2Cl_2. Potentials are *versus* ferrocenium/ferrocene (Fc^+/Fc).

3.3. Electrochemical properties

The N,C,S-tridentate ligand L^{NCS} and related ligands tend to stabilize the higher oxidation states of iron complexes (Masuda *et al.*, 2020; Nakae *et al.*, 2018). Fig. 6 shows the cyclic voltammograms of **1** and **2** in CH_2Cl_2. Measurements were performed in a 5.0×10^{-4} *M* (1 *M* = 1 mol dm^{-3}) solution containing Bu_4NPF_6 (0.1 *M*), at a scan rate of 0.1 V s^{-1}. The working electrode was a glassy carbon disk electrode with a diameter of 3 mm, the auxiliary electrode was a platinum wire, and the reference electrode was a Ag/Ag^+ (0.010 *M* $AgNO_3$) electrode. In the scanned potential range of −1.0 to 0.6 V *versus* ferrocenium/ferrocene (Fc^+/Fc), overlapping anodic peaks were observed at 0.0 and 0.23 V, which revealed that complex **1** can be oxidized at low potentials. On the reverse scan, cathodic waves were observed at 0.1 V and in the more negative region. The reverse scan from 0.1 V revealed the irreversible nature of the first oxidation process. The cathodic currents in the range of −0.9 to −1.6 V are dependent on the switching potentials, implying that the oxidized species are reduced in this potential region.

The anodic scan to 1.3 V revealed an anodic peak at 0.86 V, similar to that observed for the ligand precursor **2**. A possible

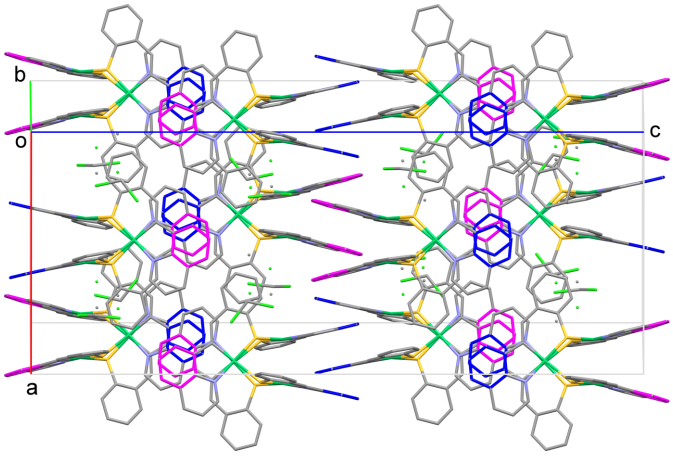


Figure 5
The crystal packing of the CH_2Cl_2 solvate of **1**. H atoms have been omitted for clarity. The C9–C14 and C26–C31 rings associated with intermolecular π–π stacking interactions are shown in blue and magenta, respectively.

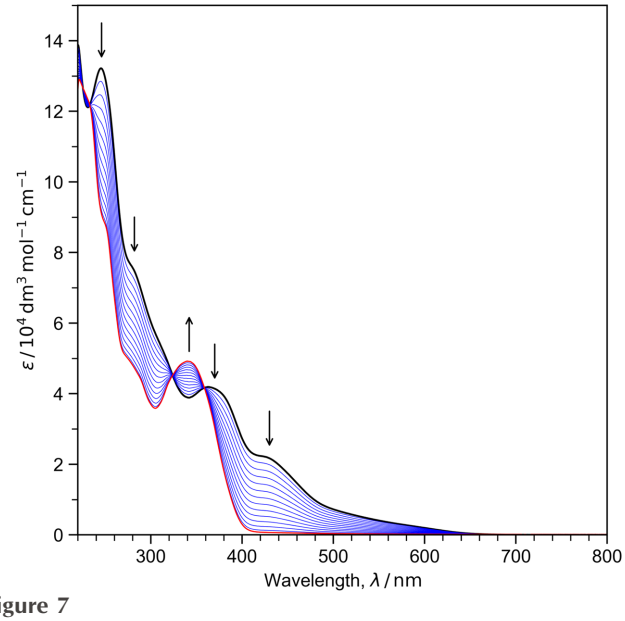


Figure 7
Absorption spectral changes of a CH_2Cl_2 solution of **1** prepared under ambient conditions (26 °C, 130 min). The black and red lines represent the initial and final spectra, respectively. The spectra were recorded every 10 min (blue lines).

explanation for these results is that the oxidation processes induce the reductive elimination of L^{NCS} to form **2** *via* the cleavage of inter-unit Ni—S bonds. Furthermore, the multistep oxidation processes suggest the presence of the multinuclear structure of **1** in solution.

3.4. Spectroscopic features

The ^1H and $^{13}C\{^1H\}$ NMR spectra of **1** in dry $CDCl_3$ showed a set of signals corresponding to one L^{NCS} ligand, indicating that four Ni(L^{NCS}) units in **1** are equivalent in solution under inert atmospheric conditions. The vinyl proton signal of **1** (δ 5.97) showed an obvious high-field shift compared with the corresponding signal of **2** (δ 8.10). NMR monitoring at 22 °C revealed the slow decomposition of **1** to form precursor **2** (~10% conversion after 17 h under inert atmospheric conditions). A similar high-field shift was also observed in C_6D_6 (δ 6.17 for **1** and δ 8.20 for **2**). Fig. 7 shows the UV–Vis absorption spectral changes of a CH_2Cl_2 solution of **1** under ambient conditions at 26 °C. The absorption bands at around 365 and 430 nm are tentatively assigned to transitions with predominantly metal-to-ligand charge-transfer character (Huang *et al.*, 2011; Gao *et al.*, 2025). The intensities of these bands decreased with time, and the final spectrum after 130 min was largely similar to that of **2**. Much slower spectral changes were observed under inert atmospheric conditions, which is consistent with the NMR experiments.

A red–brown solution of **1** in pyridine-d_5 also showed a set of ^1H NMR signals assignable to the L^{NCS} ligand under an inert atmosphere. The high-field shift of the vinyl proton signal (δ 7.93 for **1** and δ 8.44 for **2**) is smaller than that observed in $CDCl_3$ or C_6D_6, and the overall spectrum remained unchanged for two weeks. In the absorption spectrum of a pyridine solution of **1**, the absorption bands at 387 and 468 nm disappeared within 20 min under ambient conditions at 24 °C (Fig. 8). A modest high-field shift (δ 7.07 for **1** and δ 8.31 for **2**) and similarly rapid degradation in air were also observed in a DMSO-d_6 (or DMSO) solution of **1**. These results suggest that the solution species derived from **1** in solution is stabilized by coordinating solvents and undergoes reductive elimination of L^{NCS} to generate precursor **2**. The generated nickel(0) species can be readily oxidized to Ni^{2+} in air.

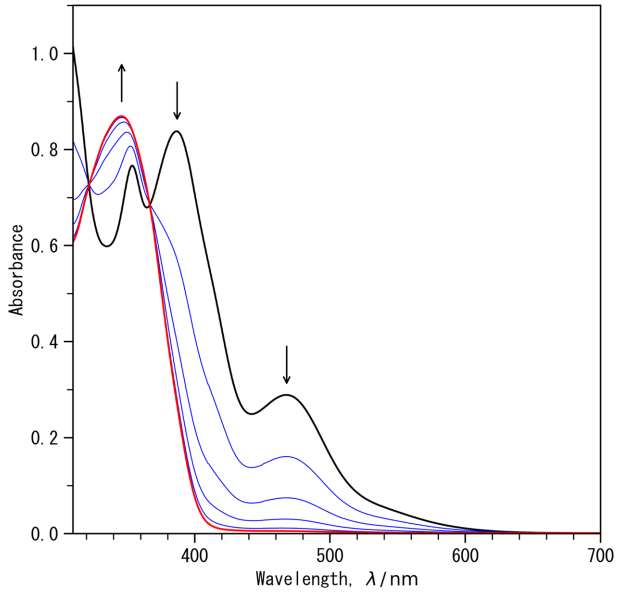


Figure 8
Absorption spectral changes of a pyridine solution of **1** under ambient conditions (24 °C, 30 min). The black line represents the spectrum under inert atmospheric conditions. After exposure to the air, the spectra were recorded every 6 min (blue lines), and the red line represents the final spectrum.

4. Conclusions

The crystal structure of the tetranuclear nickel(II) complex [{Ni(L^{NCS})}$_4$] (**1**) revealed that the N,C,S-pincer units, Ni(L^{NCS}), form a puckered Ni_4S_4 ring structure in the solid state. The inter-unit Ni—S bonds in **1** are longer than those observed in related complexes containing C,N,S- or O,N,S-tridentate ligands, presumably because of the stronger *trans* influence of the central C-donor atom in L^{NCS}. The NMR spectra and cyclic voltammograms of **1** suggest that the tetranuclear structure is retained in non-coordinating solvents, although **1** is sensitive to oxygen, particularly in the presence of coordinating solvents. On the other hand, complex **1** can be handled in air in the solid state and could potentially serve as a nickel(0) precursor.

Funding information

Funding for this research was provided by: JSPS KAKENHI (grant No. JP23K04895).

References

Albrecht, M. & van Koten, G. (2001). *Angew. Chem. Int. Ed.* **40**, 3750–3781.
Altomare, A., Burla, M. C., Camalli, M., Cascarano, G. L., Giacovazzo, C., Guagliardi, A., Moliterni, A. G. G., Polidori, G. & Spagna, R. (1999). *J. Appl. Cryst.* **32**, 115–119.
Arora, V., Narjinari, H., Nandi, P. G. & Kumar, A. (2021). *Dalton Trans.* **50**, 3394–3428.
Ataie, S., Khanzadeh, A. & Tom Baker, R. (2025). *Dalton Trans.* **54**, 8050–8054.
Bag, J. & Pal, K. (2022). *Polyhedron* **224**, 116030.
Brodnik, H., Požgan, F. & Štefane, B. (2016). *Org. Biomol. Chem.* **14**, 1969–1981.
Chakraborty, S., Bhattacharya, P., Dai, H. & Guan, H. (2015). *Acc. Chem. Res.* **48**, 1995–2003.
Farrugia, L. J. (2012). *J. Appl. Cryst.* **45**, 849–854.
Futaki, R., Chikaraishi Kasuga, N. & Hirotsu, M. (2025). *Inorg. Chem.* **64**, 23225–23237.
Gafurov, Z. N., Kantyukov, A. O., Kagilev, A. A., Kagileva, A. A., Sakhapov, I. F., Mikhailov, I. K. & Yakhvarov, D. G. (2021). *Molecules* **26**, 4063.
Gao, M., To, W.-P., Tong, G. S. M., Du, L., Low, K.-H., Tang, Z., Lu, W. & Che, C.-M. (2025). *Angew. Chem. Int. Ed.* **64**, e202414411.
Grove, D. M., Van Koten, G., Zoet, R., Murrall, N. W. & Welch, A. J. (1983). *J. Am. Chem. Soc.* **105**, 1379–1380.
Hirotsu, M., Santo, K., Hashimoto, H. & Kinoshita, I. (2012). *Organometallics* **31**, 7548–7557.

Hirotsu, M., Tsuboi, C., Nishioka, T. & Kinoshita, I. (2011). *Dalton Trans.* **40**, 785–787.
Hooper, R. X., Mercado, B. Q. & Holland, P. L. (2023). *Organometallics* **42**, 2019–2027.
Huang, D., Makhlynets, O. V., Tan, L. L., Lee, S. C., Rybak-Akimova, E. V. & Holm, R. H. (2011). *Inorg. Chem.* **50**, 10070–10081.
John, M. E., Koutsantonis, G. A., Dorta, R. & Stewart, S. G. (2026). *Chem. A Eur. J.* **32**, e71481.
Kawamoto, T. & Kushi, Y. (2004). *Bull. Chem. Soc. Jpn* **77**, 289–294.
Kawamoto, T., Nagasawa, I., Kuma, H. & Kushi, Y. (1996). *Inorg. Chem.* **35**, 2427–2432.
Kawamoto, T., Nagasawa, I., Kuma, H. & Kushi, Y. (1997). *Inorg. Chim. Acta* **265**, 163–167.
Kawamoto, T., Nagasawa, I., Kushi, Y. & Konno, T. (2003). *Inorg. Chim. Acta* **348**, 217–220.
Macrae, C. F., Sovago, I., Cottrell, S. J., Galek, P. T. A., McCabe, P., Pidcock, E., Platings, M., Shields, G. P., Stevens, J. S., Towler, M. & Wood, P. A. (2020). *J. Appl. Cryst.* **53**, 226–235.
Masuda, Y., Yagami, Y., Nakazawa, K. & Hirotsu, M. (2020). *Organometallics* **39**, 4051–4060.
Matsunaga, T., Kinoshita, I. & Hirotsu, M. (2017). *Organometallics* **36**, 2228–2236.
Moosun, S. B., Bhowon, M. G., Hosten, E. C. & Jhaumeer-Laulloo, S. (2016). *J. Coord. Chem.* **69**, 2736–2753.
Moreth, D., Cappellari, M. V., Müller, A., Oster, A., Schwab, D., Doltsinis, N. L., Strassert, C. A. & Schatzschneider, U. (2025). *Inorg. Chem.* **64**, 4223–4235.
Moulton, C. J. & Shaw, B. L. (1976). *J. Chem. Soc. Dalton Trans.* pp. 1020–1024.
Nakae, T., Hirotsu, M. & Nakajima, H. (2018). *Inorg. Chem.* **57**, 8615–8626.
Niu, J.-L., Hao, X.-Q., Gong, J.-F. & Song, M.-P. (2011). *Dalton Trans.* **40**, 5135–5150.
Rigaku (1998). *REQAB*. Rigaku Corporation, Tokyo, Japan.
Rigaku (2008). *CrystalClear*. Rigaku Corporation, Tokyo, Japan.
Roy, N., Sproules, S., Bothe, E., Weyhermüller, T. & Wieghardt, K. (2009). *Eur. J. Inorg. Chem.* **2009**, 2655–2663.
Sheldrick, G. M. (2015). *Acta Cryst.* C**71**, 3–8.
Shibue, M., Hirotsu, M., Nishioka, T. & Kinoshita, I. (2008). *Organometallics* **27**, 4475–4483.
van Koten, G., Timmer, K., Noltes, J. G. & Spek, A. L. (1978). *J. Chem. Soc. Chem. Commun.* pp. 250–252.
Wu, S., Wu, Z., Ge, Q., Zheng, X. & Yang, Z. (2021). *Org. Biomol. Chem.* **19**, 5254–5273.

supporting information

Acta Cryst. (2026). C**82** [https://doi.org/10.1107/S2053229626011952]

Synthesis, crystal structure and solution behaviour of a tetranuclear cyclometalated nickel(II) thiolate complex with a puckered Ni_4S_4 ring

Masakazu Hirotsu, Ryota Futaki and Momoka Yasuda

Computing details

Tetrakis(μ_2-{(*Z*)-2-[2-(quinolin-8-yl)eth-1-en-2-id-1-yl]benzenethiolato(2-)-κ^4N,C^1,S:*S*}tetranickel(II) dichloromethane disolvate

Crystal data

$[Ni_4(C_{17}H_{12}NS)_4]\cdot 2CH_2Cl_2$
M_r = 1450.00
Tetragonal, $I4_1/a$
a = 16.649 (3) Å
c = 41.225 (7) Å
V = 11427 (5) Å^3
Z = 8
$F(000)$ = 5920
D_x = 1.686 Mg m^{-3}
Mo $K\alpha$ radiation, λ = 0.71075 Å
Cell parameters from 12570 reflections
θ = 3.1–27.5°
μ = 1.68 mm^{-1}
T = 120 K
Prism, brown
0.07 × 0.06 × 0.04 mm

Data collection

Rigaku AFC11 with Saturn 724+ CCD diffractometer
Radiation source: Rotating Anode
Detector resolution: 28.5714 pixels mm^{-1}
ω scans
Absorption correction: multi-scan (REQAB; Rigaku, 1998)
T_{min} = 0.902, T_{max} = 1.000
93479 measured reflections
6553 independent reflections
5818 reflections with $I > 2\sigma(I)$
R_{int} = 0.054
θ_{max} = 27.5°, θ_{min} = 3.1°
h = −21→21
k = −21→21
l = −53→53

Refinement

Refinement on F^2
Least-squares matrix: full
$R[F^2 > 2\sigma(F^2)]$ = 0.057
$wR(F^2)$ = 0.151
S = 1.14
6553 reflections
408 parameters
2 restraints
Primary atom site location: structure-invariant direct methods
Hydrogen site location: mixed
H atoms treated by a mixture of independent and constrained refinement
$w = 1/[\sigma^2(F_o^2) + (0.0799P)^2 + 32.993P]$ where $P = (F_o^2 + 2F_c^2)/3$
$(\Delta/\sigma)_{max}$ = 0.002
$\Delta\rho_{max}$ = 1.63 e Å^{-3}
$\Delta\rho_{min}$ = −0.70 e Å^{-3}

Special details

Geometry. All esds (except the esd in the dihedral angle between two l.s. planes) are estimated using the full covariance matrix. The cell esds are taken into account individually in the estimation of esds in distances, angles and torsion angles; correlations between esds in cell parameters are only used when they are defined by crystal symmetry. An approximate (isotropic) treatment of cell esds is used for estimating esds involving l.s. planes.

Fractional atomic coordinates and isotropic or equivalent isotropic displacement parameters (Å²)

	x	*y*	*z*	U_{iso}*/U_{eq}	Occ. (<1)
Ni1	0.52197 (2)	0.33626 (2)	0.66106 (2)	0.01694 (13)	
Ni2	0.58613 (2)	0.22942 (2)	0.58154 (2)	0.01686 (13)	
Cl1	0.78353 (7)	0.50018 (7)	0.67290 (3)	0.0473 (3)	
Cl2A	0.72579 (12)	0.52298 (12)	0.60607 (3)	0.0654 (5)	0.85
Cl2B	0.7705 (7)	0.4741 (6)	0.60807 (19)	0.065 (3)	0.15
S1	0.61194 (4)	0.31258 (5)	0.62553 (2)	0.01902 (18)	
S2	0.56202 (4)	0.13972 (4)	0.61710 (2)	0.01850 (17)	
N1	0.44142 (16)	0.36724 (15)	0.69251 (6)	0.0191 (5)	
N2	0.62117 (15)	0.30878 (16)	0.55025 (6)	0.0196 (5)	
C1	0.70593 (18)	0.28064 (19)	0.64002 (8)	0.0213 (6)	
C2	0.7612 (2)	0.2506 (2)	0.61727 (8)	0.0268 (7)	
H2	0.745798	0.245700	0.595172	0.032*	
C3	0.8378 (2)	0.2281 (2)	0.62668 (9)	0.0295 (7)	
H3	0.874122	0.206285	0.611257	0.035*	
C4	0.8611 (2)	0.2376 (2)	0.65881 (9)	0.0314 (8)	
H4	0.914167	0.224050	0.665266	0.038*	
C5	0.8072 (2)	0.2667 (2)	0.68132 (8)	0.0262 (7)	
H5	0.823941	0.272466	0.703220	0.031*	
C6	0.72808 (19)	0.28804 (19)	0.67290 (8)	0.0221 (6)	
C7	0.67374 (19)	0.31547 (19)	0.69796 (7)	0.0225 (6)	
H7	0.697528	0.321739	0.718755	0.027*	
C8	0.59509 (19)	0.33353 (18)	0.69663 (7)	0.0201 (6)	
C9	0.47151 (19)	0.37610 (18)	0.72353 (7)	0.0210 (6)	
C10	0.5541 (2)	0.35948 (19)	0.72674 (8)	0.0226 (6)	
C11	0.5870 (2)	0.3695 (2)	0.75738 (8)	0.0280 (7)	
H11	0.642385	0.358394	0.760657	0.034*	
C12	0.5400 (2)	0.3959 (2)	0.78377 (8)	0.0324 (8)	
H12	0.564759	0.403626	0.804296	0.039*	
C13	0.4602 (2)	0.4106 (2)	0.78058 (8)	0.0297 (7)	
H13	0.429517	0.427507	0.798755	0.036*	
C14	0.4230 (2)	0.4005 (2)	0.74982 (8)	0.0237 (7)	
C15	0.3408 (2)	0.4142 (2)	0.74370 (8)	0.0270 (7)	
H15	0.306084	0.430388	0.760782	0.032*	
C16	0.3114 (2)	0.4040 (2)	0.71292 (8)	0.0260 (7)	
H16	0.256022	0.412671	0.708572	0.031*	
C17	0.36372 (19)	0.3807 (2)	0.68774 (8)	0.0229 (6)	
C18	0.53356 (18)	0.04493 (18)	0.60295 (7)	0.0201 (6)	
C19	0.5101 (2)	−0.0128 (2)	0.62587 (8)	0.0261 (7)	
H19	0.505865	0.002263	0.648027	0.031*	

C20	0.4931 (2)	−0.0908 (2)	0.61703 (9)	0.0293 (7)	
H20	0.477229	−0.128900	0.632944	0.035*	
C21	0.4993 (2)	−0.1133 (2)	0.58449 (9)	0.0302 (8)	
H21	0.488628	−0.167148	0.578167	0.036*	
C22	0.5211 (2)	−0.05687 (19)	0.56158 (8)	0.0240 (6)	
H22	0.524728	−0.072804	0.539495	0.029*	
C23	0.53825 (18)	0.02350 (19)	0.56976 (8)	0.0210 (6)	
C24	0.56224 (19)	0.07822 (19)	0.54427 (7)	0.0213 (6)	
H24	0.564380	0.055304	0.523183	0.026*	
C25	0.58208 (18)	0.15679 (19)	0.54579 (7)	0.0196 (6)	
C26	0.63132 (18)	0.27838 (19)	0.51947 (7)	0.0205 (6)	
C27	0.61179 (18)	0.19633 (19)	0.51597 (7)	0.0198 (6)	
C28	0.6237 (2)	0.1625 (2)	0.48571 (8)	0.0260 (7)	
H28	0.610735	0.107562	0.482407	0.031*	
C29	0.6549 (2)	0.2079 (2)	0.45957 (8)	0.0298 (7)	
H29	0.663364	0.182558	0.439210	0.036*	
C30	0.6730 (2)	0.2871 (2)	0.46304 (8)	0.0294 (7)	
H30	0.693335	0.316918	0.445192	0.035*	
C31	0.6611 (2)	0.3250 (2)	0.49367 (8)	0.0239 (7)	
C32	0.6786 (2)	0.4069 (2)	0.49981 (8)	0.0282 (7)	
H32	0.698713	0.440564	0.483060	0.034*	
C33	0.6658 (2)	0.4368 (2)	0.53041 (8)	0.0266 (7)	
H33	0.676198	0.491751	0.534929	0.032*	
C34	0.6371 (2)	0.38572 (19)	0.55516 (8)	0.0235 (6)	
C35A	0.7022 (3)	0.5164 (3)	0.64696 (13)	0.0434 (12)	0.85
H35A	0.663244	0.472103	0.649948	0.052*	0.85
H35B	0.675150	0.566833	0.653543	0.052*	0.85
C35B	0.7155 (13)	0.4817 (19)	0.6425 (4)	0.0434 (12)	0.15
H35C	0.685945	0.431115	0.646660	0.052*	0.15
H35D	0.676329	0.526181	0.640730	0.052*	0.15
H17	0.3469 (18)	0.3742 (17)	0.6651 (7)	0.000 (7)*	
H34	0.628 (2)	0.405 (2)	0.5775 (9)	0.018 (9)*	

Atomic displacement parameters (Å²)

	U^{11}	U^{22}	U^{33}	U^{12}	U^{13}	U^{23}
Ni1	0.0189 (2)	0.0188 (2)	0.0132 (2)	0.00020 (14)	−0.00029 (13)	−0.00131 (13)
Ni2	0.0196 (2)	0.0180 (2)	0.0130 (2)	−0.00020 (14)	0.00159 (13)	0.00020 (13)
Cl1	0.0503 (6)	0.0456 (6)	0.0459 (6)	0.0006 (5)	−0.0061 (5)	0.0051 (5)
Cl2A	0.0843 (12)	0.0812 (12)	0.0307 (7)	−0.0468 (10)	−0.0022 (7)	−0.0014 (7)
Cl2B	0.095 (7)	0.069 (6)	0.030 (4)	−0.049 (5)	−0.006 (4)	0.009 (4)
S1	0.0200 (4)	0.0220 (4)	0.0151 (3)	0.0003 (3)	0.0007 (3)	−0.0020 (3)
S2	0.0218 (4)	0.0198 (4)	0.0139 (3)	−0.0007 (3)	0.0012 (3)	0.0008 (3)
N1	0.0231 (13)	0.0175 (12)	0.0166 (12)	−0.0009 (10)	0.0016 (10)	−0.0002 (9)
N2	0.0208 (13)	0.0220 (13)	0.0162 (12)	0.0011 (10)	−0.0002 (10)	−0.0012 (10)
C1	0.0201 (15)	0.0222 (15)	0.0216 (15)	−0.0007 (12)	−0.0004 (12)	0.0005 (12)
C2	0.0261 (17)	0.0332 (18)	0.0211 (16)	0.0006 (14)	0.0040 (12)	−0.0023 (13)
C3	0.0236 (17)	0.0353 (19)	0.0296 (18)	0.0051 (14)	0.0069 (13)	0.0002 (14)

C4	0.0205 (16)	0.037 (2)	0.037 (2)	0.0019 (14)	−0.0005 (14)	0.0024 (15)
C5	0.0242 (16)	0.0289 (17)	0.0254 (16)	−0.0012 (13)	−0.0035 (13)	0.0020 (13)
C6	0.0234 (16)	0.0200 (15)	0.0228 (15)	−0.0014 (12)	−0.0003 (12)	−0.0006 (12)
C7	0.0242 (16)	0.0266 (16)	0.0168 (14)	−0.0035 (12)	−0.0064 (12)	−0.0012 (12)
C8	0.0249 (16)	0.0187 (14)	0.0166 (14)	−0.0033 (12)	−0.0013 (11)	0.0000 (11)
C9	0.0267 (16)	0.0202 (15)	0.0159 (14)	0.0003 (12)	0.0003 (12)	0.0010 (11)
C10	0.0272 (16)	0.0214 (15)	0.0193 (15)	0.0012 (12)	−0.0006 (12)	0.0005 (12)
C11	0.0319 (18)	0.0344 (19)	0.0175 (15)	0.0026 (14)	−0.0050 (13)	−0.0002 (13)
C12	0.044 (2)	0.0361 (19)	0.0173 (16)	0.0062 (16)	−0.0032 (14)	−0.0033 (14)
C13	0.042 (2)	0.0322 (18)	0.0150 (15)	0.0037 (15)	0.0037 (13)	−0.0028 (13)
C14	0.0301 (17)	0.0261 (16)	0.0151 (14)	0.0008 (13)	0.0047 (12)	−0.0002 (12)
C15	0.0305 (18)	0.0295 (17)	0.0209 (15)	0.0016 (14)	0.0081 (13)	−0.0004 (13)
C16	0.0218 (16)	0.0294 (17)	0.0269 (17)	−0.0007 (13)	0.0044 (13)	0.0015 (13)
C17	0.0230 (16)	0.0262 (16)	0.0194 (15)	0.0010 (12)	0.0005 (12)	0.0002 (12)
C18	0.0198 (14)	0.0200 (14)	0.0204 (15)	0.0009 (11)	0.0022 (11)	0.0006 (11)
C19	0.0308 (17)	0.0260 (16)	0.0215 (15)	−0.0005 (13)	−0.0007 (13)	0.0036 (13)
C20	0.038 (2)	0.0240 (17)	0.0260 (17)	−0.0032 (14)	−0.0009 (14)	0.0086 (13)
C21	0.039 (2)	0.0195 (16)	0.0319 (19)	−0.0027 (14)	−0.0005 (15)	−0.0012 (13)
C22	0.0283 (16)	0.0222 (15)	0.0214 (15)	−0.0011 (12)	0.0004 (12)	−0.0049 (12)
C23	0.0194 (14)	0.0219 (15)	0.0216 (15)	0.0016 (11)	0.0001 (11)	−0.0019 (12)
C24	0.0239 (15)	0.0255 (16)	0.0145 (13)	0.0014 (12)	0.0003 (11)	−0.0025 (11)
C25	0.0198 (14)	0.0265 (16)	0.0124 (13)	0.0025 (12)	−0.0002 (11)	−0.0009 (11)
C26	0.0203 (15)	0.0234 (15)	0.0179 (14)	0.0015 (12)	−0.0014 (11)	0.0017 (11)
C27	0.0196 (14)	0.0234 (15)	0.0165 (14)	0.0000 (12)	0.0010 (11)	0.0008 (11)
C28	0.0305 (18)	0.0273 (17)	0.0203 (16)	−0.0004 (13)	0.0023 (13)	−0.0008 (13)
C29	0.0337 (19)	0.040 (2)	0.0162 (15)	−0.0022 (15)	0.0055 (13)	−0.0021 (13)
C30	0.0297 (17)	0.044 (2)	0.0149 (15)	0.0002 (15)	0.0045 (12)	0.0080 (14)
C31	0.0257 (16)	0.0271 (17)	0.0190 (15)	−0.0018 (13)	−0.0007 (12)	0.0034 (12)
C32	0.0300 (18)	0.0291 (18)	0.0254 (17)	−0.0001 (14)	−0.0001 (13)	0.0099 (13)
C33	0.0328 (18)	0.0203 (15)	0.0268 (17)	−0.0004 (13)	0.0002 (13)	0.0040 (13)
C34	0.0249 (16)	0.0233 (16)	0.0223 (16)	0.0004 (12)	−0.0010 (12)	0.0021 (12)
C35A	0.054 (3)	0.030 (3)	0.046 (3)	−0.015 (2)	0.004 (2)	−0.009 (2)
C35B	0.054 (3)	0.030 (3)	0.046 (3)	−0.015 (2)	0.004 (2)	−0.009 (2)

Geometric parameters (Å, º)

Ni1—C8	1.906 (3)	C13—C14	1.421 (5)
Ni1—N1	1.935 (3)	C13—H13	0.9500
Ni1—S1	2.1320 (9)	C14—C15	1.411 (5)
Ni1—S2^{i}	2.3241 (9)	C15—C16	1.371 (5)
Ni1—Ni1^{i}	2.9639 (9)	C15—H15	0.9500
Ni2—C25	1.908 (3)	C16—C17	1.410 (4)
Ni2—N2	1.936 (3)	C16—H16	0.9500
Ni2—S2	2.1308 (8)	C17—H17	0.98 (3)
Ni2—S1	2.3217 (9)	C18—C19	1.403 (4)
Ni2—Ni2^{i}	2.9486 (9)	C18—C23	1.416 (4)
Cl1—C35B	1.718 (18)	C19—C20	1.378 (5)
Cl1—C35A	1.747 (5)	C19—H19	0.9500

Cl2A—C35A	1.734 (5)	C20—C21	1.397 (5)
Cl2B—C35B	1.693 (18)	C20—H20	0.9500
S1—C1	1.757 (3)	C21—C22	1.381 (5)
S2—C18	1.748 (3)	C21—H21	0.9500
N1—C17	1.328 (4)	C22—C23	1.409 (4)
N1—C9	1.381 (4)	C22—H22	0.9500
N2—C34	1.324 (4)	C23—C24	1.447 (4)
N2—C26	1.376 (4)	C24—C25	1.351 (4)
C1—C2	1.406 (4)	C24—H24	0.9500
C1—C6	1.410 (4)	C25—C27	1.480 (4)
C2—C3	1.384 (5)	C26—C31	1.407 (4)
C2—H2	0.9500	C26—C27	1.412 (4)
C3—C4	1.389 (5)	C27—C28	1.383 (4)
C3—H3	0.9500	C28—C29	1.415 (5)
C4—C5	1.379 (5)	C28—H28	0.9500
C4—H4	0.9500	C29—C30	1.360 (5)
C5—C6	1.407 (5)	C29—H29	0.9500
C5—H5	0.9500	C30—C31	1.425 (5)
C6—C7	1.447 (4)	C30—H30	0.9500
C7—C8	1.345 (5)	C31—C32	1.418 (5)
C7—H7	0.9500	C32—C33	1.373 (5)
C8—C10	1.481 (4)	C32—H32	0.9500
C9—C10	1.408 (5)	C33—C34	1.411 (4)
C9—C14	1.411 (4)	C33—H33	0.9500
C10—C11	1.387 (4)	C34—H34	0.99 (4)
C11—C12	1.411 (5)	C35A—H35A	0.9900
C11—H11	0.9500	C35A—H35B	0.9900
C12—C13	1.356 (5)	C35B—H35C	0.9900
C12—H12	0.9500	C35B—H35D	0.9900

C8—Ni1—N1	86.20 (12)	C9—C14—C13	118.0 (3)
C8—Ni1—S1	94.33 (10)	C16—C15—C14	119.5 (3)
N1—Ni1—S1	175.18 (8)	C16—C15—H15	120.3
C8—Ni1—S2^{i}	171.21 (9)	C14—C15—H15	120.3
N1—Ni1—S2^{i}	93.42 (8)	C15—C16—C17	119.7 (3)
S1—Ni1—S2^{i}	85.33 (3)	C15—C16—H16	120.2
C8—Ni1—Ni1^{i}	97.74 (9)	C17—C16—H16	120.2
N1—Ni1—Ni1^{i}	95.00 (8)	N1—C17—C16	122.7 (3)
S1—Ni1—Ni1^{i}	89.67 (3)	N1—C17—H17	113.6 (17)
S2^{i}—Ni1—Ni1^{i}	91.04 (2)	C16—C17—H17	123.7 (18)
C25—Ni2—N2	85.90 (12)	C19—C18—C23	119.5 (3)
C25—Ni2—S2	94.62 (10)	C19—C18—S2	118.0 (2)
N2—Ni2—S2	173.32 (8)	C23—C18—S2	122.3 (2)
C25—Ni2—S1	171.13 (9)	C20—C19—C18	121.7 (3)
N2—Ni2—S1	93.31 (8)	C20—C19—H19	119.2
S2—Ni2—S1	85.15 (3)	C18—C19—H19	119.2
C25—Ni2—Ni2^{i}	96.48 (9)	C19—C20—C21	119.4 (3)
N2—Ni2—Ni2^{i}	97.73 (8)	C19—C20—H20	120.3

S2—Ni2—Ni2^{i}	88.84 (3)	C21—C20—H20	120.3
S1—Ni2—Ni2^{i}	92.38 (2)	C22—C21—C20	119.6 (3)
C1—S1—Ni1	116.61 (11)	C22—C21—H21	120.2
C1—S1—Ni2	104.47 (11)	C20—C21—H21	120.2
Ni1—S1—Ni2	121.13 (4)	C21—C22—C23	122.4 (3)
C18—S2—Ni2	117.02 (11)	C21—C22—H22	118.8
C18—S2—Ni1^{i}	104.62 (10)	C23—C22—H22	118.8
Ni2—S2—Ni1^{i}	121.96 (4)	C22—C23—C18	117.4 (3)
C17—N1—C9	118.2 (3)	C22—C23—C24	118.7 (3)
C17—N1—Ni1	128.4 (2)	C18—C23—C24	123.9 (3)
C9—N1—Ni1	113.4 (2)	C25—C24—C23	130.1 (3)
C34—N2—C26	118.2 (3)	C25—C24—H24	115.0
C34—N2—Ni2	128.2 (2)	C23—C24—H24	115.0
C26—N2—Ni2	113.6 (2)	C24—C25—C27	118.3 (3)
C2—C1—C6	120.1 (3)	C24—C25—Ni2	131.2 (2)
C2—C1—S1	117.6 (2)	C27—C25—Ni2	110.4 (2)
C6—C1—S1	122.2 (2)	N2—C26—C31	122.5 (3)
C3—C2—C1	120.8 (3)	N2—C26—C27	114.9 (3)
C3—C2—H2	119.6	C31—C26—C27	122.5 (3)
C1—C2—H2	119.6	C28—C27—C26	116.9 (3)
C2—C3—C4	119.6 (3)	C28—C27—C25	128.1 (3)
C2—C3—H3	120.2	C26—C27—C25	115.0 (3)
C4—C3—H3	120.2	C27—C28—C29	121.5 (3)
C5—C4—C3	120.0 (3)	C27—C28—H28	119.3
C5—C4—H4	120.0	C29—C28—H28	119.3
C3—C4—H4	120.0	C30—C29—C28	121.3 (3)
C4—C5—C6	122.1 (3)	C30—C29—H29	119.4
C4—C5—H5	118.9	C28—C29—H29	119.4
C6—C5—H5	118.9	C29—C30—C31	119.4 (3)
C5—C6—C1	117.4 (3)	C29—C30—H30	120.3
C5—C6—C7	119.3 (3)	C31—C30—H30	120.3
C1—C6—C7	123.4 (3)	C26—C31—C32	117.9 (3)
C8—C7—C6	130.6 (3)	C26—C31—C30	118.4 (3)
C8—C7—H7	114.7	C32—C31—C30	123.7 (3)
C6—C7—H7	114.7	C33—C32—C31	118.7 (3)
C7—C8—C10	118.7 (3)	C33—C32—H32	120.6
C7—C8—Ni1	131.2 (2)	C31—C32—H32	120.6
C10—C8—Ni1	110.1 (2)	C32—C33—C34	119.9 (3)
N1—C9—C10	114.8 (3)	C32—C33—H33	120.0
N1—C9—C14	122.3 (3)	C34—C33—H33	120.0
C10—C9—C14	122.9 (3)	N2—C34—C33	122.7 (3)
C11—C10—C9	116.6 (3)	N2—C34—H34	115 (2)
C11—C10—C8	128.0 (3)	C33—C34—H34	122 (2)
C9—C10—C8	115.4 (3)	Cl2A—C35A—Cl1	115.4 (3)
C10—C11—C12	121.3 (3)	Cl2A—C35A—H35A	108.4
C10—C11—H11	119.3	Cl1—C35A—H35A	108.4
C12—C11—H11	119.3	Cl2A—C35A—H35B	108.4
C13—C12—C11	121.6 (3)	Cl1—C35A—H35B	108.4

C13—C12—H12	119.2	H35A—C35A—H35B	107.5
C11—C12—H12	119.2	Cl2B—C35B—Cl1	105.6 (11)
C12—C13—C14	119.5 (3)	Cl2B—C35B—H35C	110.6
C12—C13—H13	120.3	Cl1—C35B—H35C	110.6
C14—C13—H13	120.3	Cl2B—C35B—H35D	110.6
C15—C14—C9	117.7 (3)	Cl1—C35B—H35D	110.6
C15—C14—C13	124.3 (3)	H35C—C35B—H35D	108.8

Ni1—S1—C1—C2	168.5 (2)	Ni2—S2—C18—C19	−174.1 (2)
Ni2—S1—C1—C2	31.9 (3)	Ni1^{i}—S2—C18—C19	−35.8 (3)
Ni1—S1—C1—C6	−14.6 (3)	Ni2—S2—C18—C23	9.9 (3)
Ni2—S1—C1—C6	−151.2 (2)	Ni1^{i}—S2—C18—C23	148.2 (2)
C6—C1—C2—C3	−0.1 (5)	C23—C18—C19—C20	1.5 (5)
S1—C1—C2—C3	176.8 (3)	S2—C18—C19—C20	−174.7 (3)
C1—C2—C3—C4	−2.0 (6)	C18—C19—C20—C21	0.1 (6)
C2—C3—C4—C5	2.2 (6)	C19—C20—C21—C22	−1.1 (6)
C3—C4—C5—C6	−0.4 (6)	C20—C21—C22—C23	0.5 (6)
C4—C5—C6—C1	−1.6 (5)	C21—C22—C23—C18	1.0 (5)
C4—C5—C6—C7	177.8 (3)	C21—C22—C23—C24	178.7 (3)
C2—C1—C6—C5	1.9 (5)	C19—C18—C23—C22	−1.9 (4)
S1—C1—C6—C5	−174.9 (2)	S2—C18—C23—C22	174.0 (2)
C2—C1—C6—C7	−177.5 (3)	C19—C18—C23—C24	−179.6 (3)
S1—C1—C6—C7	5.7 (5)	S2—C18—C23—C24	−3.6 (4)
C5—C6—C7—C8	−174.6 (3)	C22—C23—C24—C25	−179.5 (3)
C1—C6—C7—C8	4.8 (6)	C18—C23—C24—C25	−1.9 (5)
C6—C7—C8—C10	179.2 (3)	C23—C24—C25—C27	174.4 (3)
C6—C7—C8—Ni1	−3.6 (6)	C23—C24—C25—Ni2	−0.7 (5)
C17—N1—C9—C10	178.9 (3)	C34—N2—C26—C31	2.9 (5)
Ni1—N1—C9—C10	−1.3 (3)	Ni2—N2—C26—C31	−176.1 (2)
C17—N1—C9—C14	−1.5 (5)	C34—N2—C26—C27	−178.9 (3)
Ni1—N1—C9—C14	178.3 (2)	Ni2—N2—C26—C27	2.2 (3)
N1—C9—C10—C11	178.5 (3)	N2—C26—C27—C28	−177.8 (3)
C14—C9—C10—C11	−1.0 (5)	C31—C26—C27—C28	0.5 (5)
N1—C9—C10—C8	−1.3 (4)	N2—C26—C27—C25	1.1 (4)
C14—C9—C10—C8	179.2 (3)	C31—C26—C27—C25	179.4 (3)
C7—C8—C10—C11	1.2 (5)	C24—C25—C27—C28	−1.1 (5)
Ni1—C8—C10—C11	−176.6 (3)	Ni2—C25—C27—C28	174.9 (3)
C7—C8—C10—C9	−179.0 (3)	C24—C25—C27—C26	−180.0 (3)
Ni1—C8—C10—C9	3.2 (3)	Ni2—C25—C27—C26	−3.9 (3)
C9—C10—C11—C12	−0.7 (5)	C26—C27—C28—C29	0.6 (5)
C8—C10—C11—C12	179.1 (3)	C25—C27—C28—C29	−178.2 (3)
C10—C11—C12—C13	1.7 (6)	C27—C28—C29—C30	−1.2 (6)
C11—C12—C13—C14	−1.0 (6)	C28—C29—C30—C31	0.7 (5)
N1—C9—C14—C15	1.5 (5)	N2—C26—C31—C32	−2.1 (5)
C10—C9—C14—C15	−179.0 (3)	C27—C26—C31—C32	179.8 (3)
N1—C9—C14—C13	−177.8 (3)	N2—C26—C31—C30	177.2 (3)
C10—C9—C14—C13	1.7 (5)	C27—C26—C31—C30	−1.0 (5)
C12—C13—C14—C15	−179.8 (3)	C29—C30—C31—C26	0.4 (5)

C12—C13—C14—C9	−0.6 (5)	C29—C30—C31—C32	179.6 (3)
C9—C14—C15—C16	−0.4 (5)	C26—C31—C32—C33	0.1 (5)
C13—C14—C15—C16	178.8 (3)	C30—C31—C32—C33	−179.1 (3)
C14—C15—C16—C17	−0.5 (5)	C31—C32—C33—C34	1.1 (5)
C9—N1—C17—C16	0.5 (5)	C26—N2—C34—C33	−1.6 (5)
Ni1—N1—C17—C16	−179.2 (2)	Ni2—N2—C34—C33	177.1 (2)
C15—C16—C17—N1	0.5 (5)	C32—C33—C34—N2	−0.3 (5)

Symmetry code: (i) −*x*+1, −*y*+1/2, *z*.

Hydrogen-bond geometry (Å, º)

D—H···*A*	*D*—H	H···*A*	*D*···*A*	*D*—H···*A*
C17—H17···S2^{i}	0.98 (3)	2.50 (3)	3.182 (3)	126 (2)
C34—H34···S1	0.99 (4)	2.52 (4)	3.174 (3)	124 (3)

Symmetry code: (i) −*x*+1, −*y*+1/2, *z*.